Emerging trends in OBIC characterization technique for Wide Bandgap semiconductor devices

Dominique Planson, Camille Sonneville, Pascal Bevilacqua, Dominique Tournier

Emerging trends in OBIC characterization technique for Wide Bandgap semiconductor devices

Dominique PLANSON*, Camille SONNEVILLE,**
Pascal BEVILACQUA, Dominique TOURNIER****
*Univ Lyon, INSA Lyon, Ecole Centrale de Lyon, Université Claude Bernard Lyon 1, CNRS, Ampère, F-69621, Villeurbanne, France
dominique.planson@insa-lyon.fr
** Univ Lyon, INSA Lyon, Ecole Centrale de Lyon, Université Claude Bernard Lyon 1, CNRS, Ampère, F-69621, Villeurbanne, France
****camille.sonneville, **pascal.bevilacqua, **dominique.tournier@insa-lyon.fr**

Abstract*— Wide-bandgap semiconductors, like silicon carbide (SiC), gallium nitride (GaN), and diamond (C), outperform silicon (Si) based power electronic devices. However, the peripheral protection of these wide-bandgap devices needs to be carefully designed to handle high voltage. This article demonstrates the potential of using the OBIC (Optical Beam Induced Current) technique to analyze different protection methods' effectiveness and provide feedback to device designers regarding peripheral termination efficiency.

At the beginning, the article presents a theoretical approach to introduce the OBIC method. Subsequently, the electro-optical characterization technique is applied to high-voltage power devices within a vacuum chamber, enabling the examination of the electric field's spatial distribution in the semiconductor. The focus is on SiC devices due to their availability. Throughout the years, this technique has evolved, with advancements made in reducing spot size and enhancing sample placement precision. The article will also showcase new results obtained from components with new-generation peripheral protection.

Keywords*— optical device characterization, power devices, high voltage device, periphery protection, Silicon Carbide, OBIC.

1. Introduction

Wide Bandgap semiconductors materials like Silicon Carbide (SiC) Gallium Nitride (GaN) and Diamond (C) have excellent properties for many applications especially for high voltage devices [1][2][3].

In the near future, advanced power grids and High Voltage Direct Current (HVDC) transmission systems will increasingly rely on ultrahigh voltage devices (>10 kV) [4][5][6]. In order to fully leverage the benefits of wide-bandgap semiconductor materials and prevent premature breakdown of these high voltage devices, it is crucial to have effective peripheral protections [7][8][9]. This paper aims to demonstrate how the OBIC technique can be utilized to assess the efficiency of peripheral protection by analyzing the distribution of the electric field within the device structure, particularly at the junction periphery. The OBIC technique enables high-voltage measurements to be conducted on reverse-biased components and needs precautions such as a vacuum chamber and the transmission of the optical beam through an optical window. This paper is divided in three main sections. The first part provides a comprehensive description of the OBIC principle. The second part presents the results and analysis obtained from medium and high voltage bipolar diodes using OBIC near breakdown voltages. Finally, the last part focuses on characterizing lower voltage devices with optimized periphery protection using our enhanced setup.

2. OBIC principle

This technique has been used to investigate silicon diodes protected by field rings [10] [11]. The semiconductor device characterization process involves the utilization of a focused laser beam, as depicted in **Fig. 1**, to generate electron-hole pairs (EHPs) within the semiconductor. To

achieve a focused spot with a diameter of approximately 70 µm on the semiconductor surface, two semi-reflecting mirrors and a focusing lens are precisely controlled using Labview software in the initial setup. The high voltage device under test (DUT), as illustrated in **Fig. 2**, is positioned within a vacuum chamber and subjected to reverse biasing using a high voltage supply (FUG) with a maximum voltage of 12.5 kV.

The surface of the DUT is scanned in with a step of 10 µm under high voltage. Current is measured with a microammeter (Keithley 6485). It allows to realize mapping of the induced current in both directions (X and Y) or only lines. The intensity of the photo-generated current is related to the electric field strength and hence to the reverse voltage applied to the DUT. The OBIC setup has already been described elsewhere in [12][13].

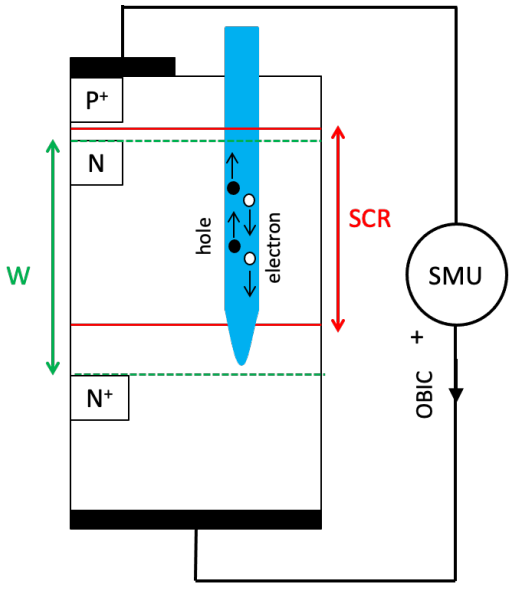

Fig. 1 Reverse-biased plane-parallel infinite PN junction. The boundaries of the space charge region (SCR) are indicated in red, while the n-epilayer has a thickness denoted as W.

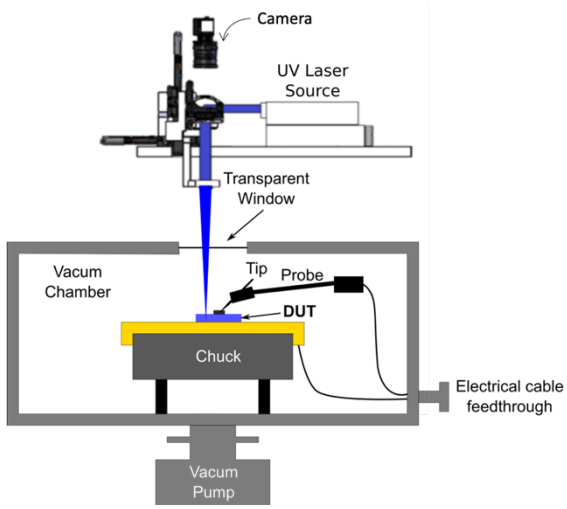

Fig. 2 Schematic of the experimental OBIC bench

Two distinct beam wavelengths can be employed for OBIC characterization, namely the green wavelength with λ=532 nm and the UV wavelength with λ=349 nm. These wavelengths are generated by two different pulsed semiconductor lasers. When it comes to SiC devices, solely the UV wavelength is utilized since its energy is greater than the energy bandgap requirement for effective characterization. This non-destructive technique allows to measure OBIC currents by scanning the outer edge of the biased diode, in order to assess the periphery protection efficiency. OBIC current increases as the electric field intensity increases in the structure. There is no OBIC current on the metallization, neither far from the periphery of the diode.

3. First measurements

A. Medium voltage PiN diodes (3.3 kV class)

The first OBIC measurements were carried out using the old test bench on medium-voltage SiC bipolar diodes (depicted in **Fig 3**).

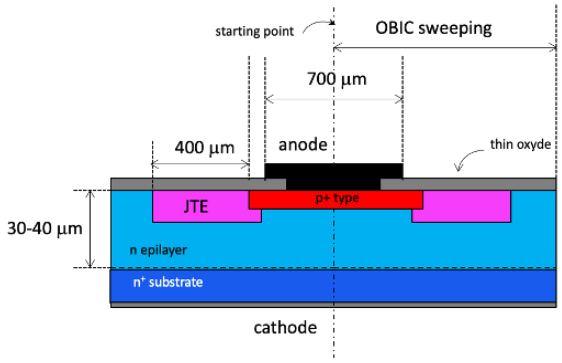

Fig. 3 Cross sectional view of the vertical PiN JTE protected diode. The zone where the OBIC measurement is performed extends from the center of the diode towards the outer edges.

Bipolar vertical diodes were designed with a voltage withstand target of 3.3 kV, for this purpose 2 doses were implemented for the JTE (Junction Termination Extension) zone. The values of the 2 doses are given in **Table 1**.

Table 1. details of the 2 doses and thicknesses

	Device #1	Device #2
JTE dose [cm^{-2}]	1.23×10^{13}	6.84×10^{12}
Epilayer thickness [µm]	40	30

Generally, the dose of JTE must be very precisely controlled, otherwise the breakdown voltage will be reduced.

OBIC measurements were carried out on both devices, Device #1 and Device #2. The reverse voltages applied varied between 800 and 2850V. For device #1 with the highest JTE dose, the increase in OBIC current is located near the edge of the JTE, as can be seen in **Fig. 4**. On the contrary, with device #2, the lowest JTE dose, the increase in OBIC current is located near the P^+/JTE zone, as can be seen in **Fig. 5**. The location of the metallization, P^+ and JTE zones is shown at the bottom of each graph.

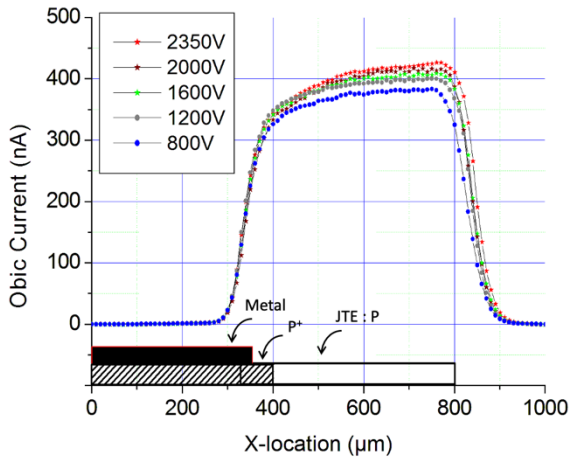

Fig. 4 OBIC current measured at different increasing voltages on device #1. A 10 µm step for the line was used.

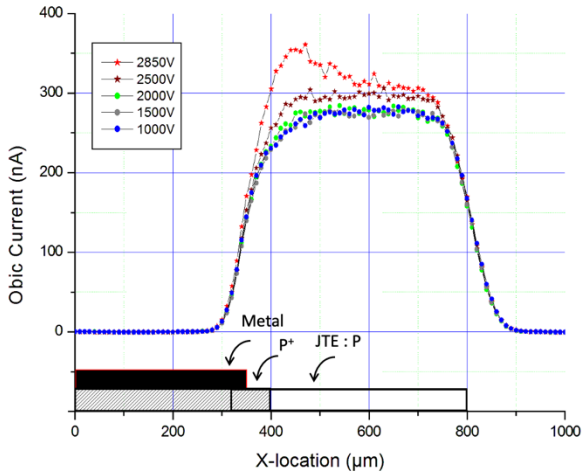

Fig. 5 OBIC current measured at different increasing voltages on device #2. A 10 µm step for the line was used.

Near breakdown voltage induces high electric field, which leads to an increase of the OBIC signal, as it can clearly be observed for device #2, this is due to a dose of JTE that is too low. Combining both results on device #1 and device #2, we can conclude that the JTE dose must be adjusted more precisely.

B. High voltage PiN diodes (10 kV class)

High voltage PiN diodes were fabricated on a 4H-SiC wafer using a 110 µm thick epilayer with a doping concentration of 7×10^{14} cm^{-3}. These diodes are MESA-JTE protected with or without JTE-ring (6 or 8 rings), as shown in **Fig. 6**.

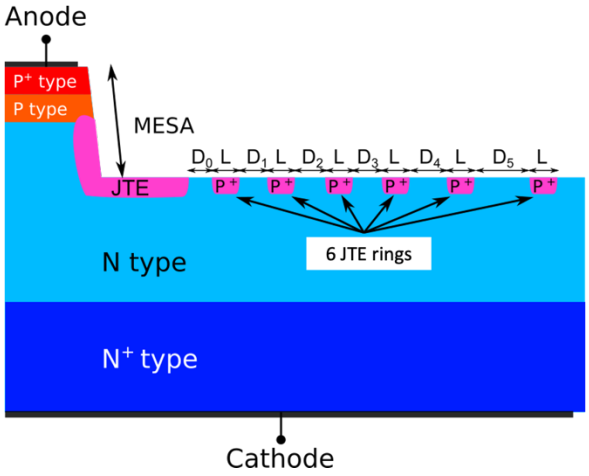

Fig. 6 Cross sectional view of the right half part of high voltage bipolar PiN diode MESA protected with 6 JTE rings.

Before conducting the OBIC measurements, reverse IV characteristics were carried out to determine the near breakdown voltage [13]. High voltage OBIC measurements were also performed in 1D-sweeping mode with a 10 µm step increment for increasing voltages. 4 kinds of diodes were measured (400 µm JTE length, 500 µm JTE length, 400 µm JTE length with 6 JTE-rings and finally 400 µm JTE length with 8 JTE-rings).

As the voltage increases closed to the breakdown voltage, one can observe in **Fig. 7 to 10** the appearance of an OBIC peak located near the P^+/JTE area. This peak is due to the electric field enhancement at the P+/JTE overlap, meaning that the JTE dose is too low. Moreover, experimental breakdown voltages are far from the theoretical breakdown voltage (10 kV) and the impact of the protection is not very clear. It may be due to interface charge near the surface of the device. In these cases, there is no influence of the JTE rings.

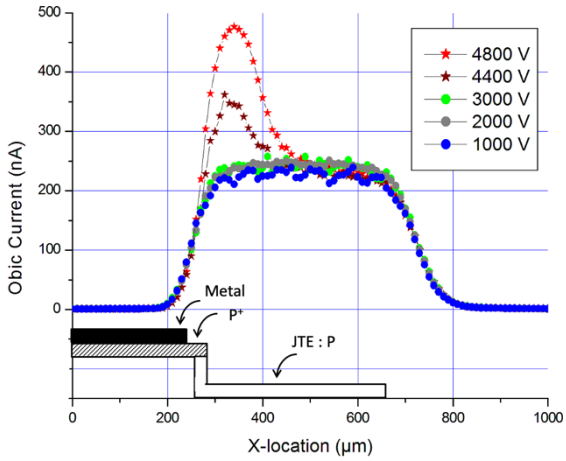

Fig. 7 1D-sweeping OBIC measurements were performed on a diode with a **400 µm MESA JTE** protection at various voltages.

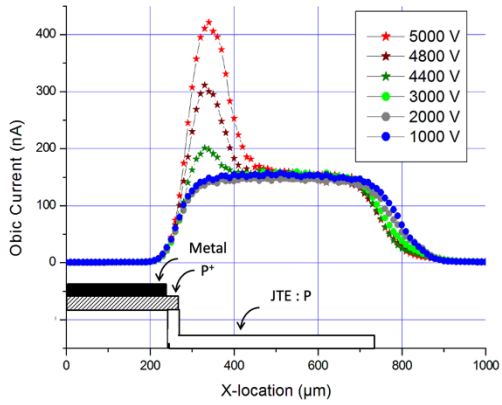

Fig. 8 1D-sweeping OBIC measurements were performed on a diode with a **500 µm MESA JTE** protection at various voltages.

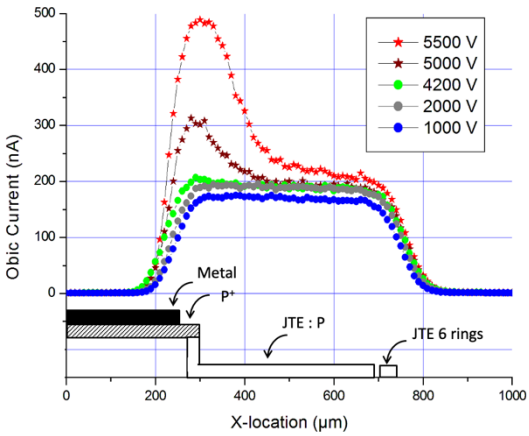

Fig. 9 1D-sweeping OBIC measurements were performed on a diode with a **400 µm + 6 rings MESA JTE** protection at various voltages.

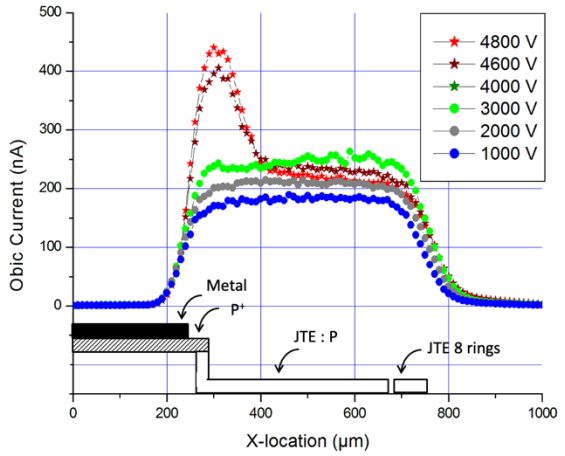

Fig. 10 1D-sweeping OBIC measurements were performed on a diode with a **400 µm + 8 rings MESA JTE** protection at various voltages.

4. Improved measurements

A. New experimental setup

In the micro-OBIC experimental setup, a 349 nm UV pulsed laser is used to generate electron-hole pairs (EHPs) as in the previous testbench. A set of properly adjusted optics (mirrors, microscope objective …) is inserted on the beam path to finally get a focused laser spot with a diameter of about 1-4 µm as shown in **Fig. 11**. The sample is placed on a motorized stage and the position of the focalization point is controlled with LabView (i.e. on X, Y, Z automatically and teta manually). The micro-OBIC setup has already been described in [14][15].

The testbench allows us to realize a spatial mapping of OBIC signal, either on a (X, Y) plane or only on X (or Y) lines. For X or Y lines, the step between two displacements of the laser beam is 200 nm instead of 10 µm, Anode-Cathode reverse biased. The DUT can be reverse biased by applying a voltage of up to 1100V using the Keithley 237 SMU (Source Measure Unit), but this is limited to 500V to prevent arcing in the air because the DUT is not under vacuum.

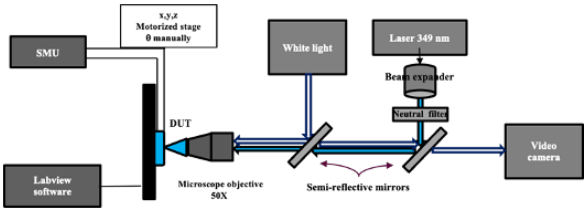

Fig. 11 Schematic representation of the enhanced micro-OBIC testbench.

B. Experimental results on 1.7 kV bipolar diode

The cross section of the DUT and its periphery is sketched in the **Fig 12**. The epilayer is 14.8 µm thick, n-type doped (6×10^{15} cm^{-3}). The main junction is realized by ion implantation, at the same time as the field rings, which were carefully designed by CALY Technologies. To avoid breakdown in air, the diode was passivated, but this passivation was removed to facilitate measurements with the UV beam [16].

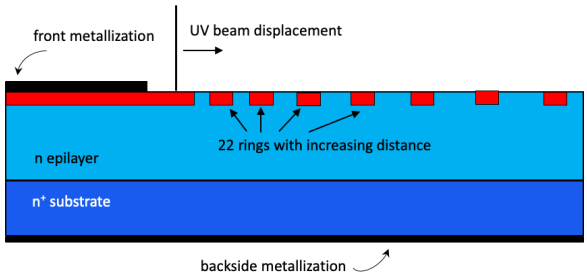

Fig. 12 Schematic cross section view of half vertical PiN diodes protected by 22 field rings.

The metallized anode contact is square-shaped, with a side length of 200 µm × 300 µm, and a corner curvature radius of 200 µm as shown in **Fig. 13**.

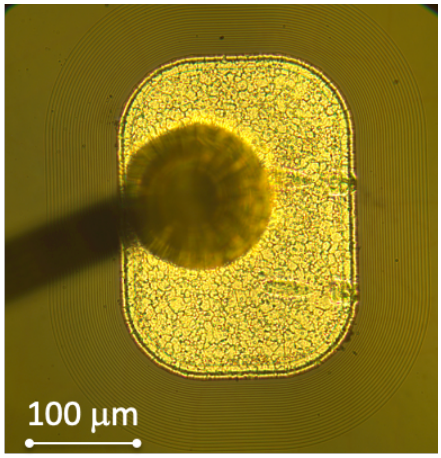

Fig. 13 Photograph of the diode with the 50 µm (diameter) gold ball bonding.

The diode is protected by 22 field rings as shown in **Fig. 12**, with increasing spacing between them (0.07 µm from one ring to the next). The distance between the main junction and the first ring is 1.2 µm. All the

rings have the same width (1.5 µm). The total length of the periphery protection is 96 µm.

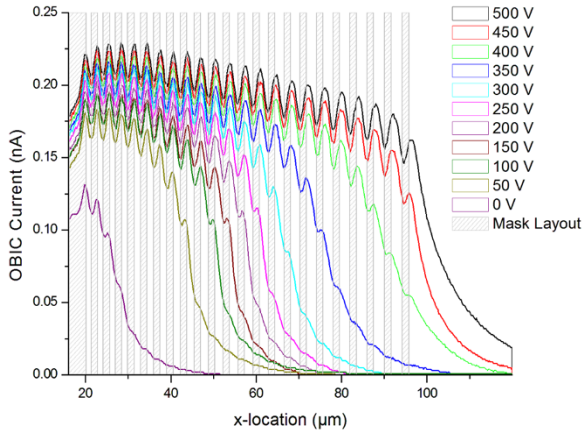

Fig. 14 OBIC currents at the periphery of the diode device at various reverse voltages (ranging from 0V up to 500V by 50V step). The mask layout with the spacing between the rings is in grey color.

By varying the reverse voltages (up to 500V) applied to the same diode and rescanning the exact sweeping, multiple OBIC currents can be compared, as illustrated in **Fig. 13**. As the reverse voltage rises, the OBIC current also increases at the same location, due to the augmentation of the electric field. Additionally, one can observe the lateral expansion of the space charge region as the reverse voltage increases, highlighting the significant contribution of the outer field rings, which attests to the efficiency of the peripheral protection design.

As the reverse voltage increase, the number of OBIC peaks increase too. From 20 µm up to 97 µm, each maximum is related to the presence of a ring as described in [16] and, more precisely, is located on the outer edge of each ring junction. As the reverse voltage increases, the presence of the rings is more clearly revealed by µ-OBIC. These measurements up to 500V, show the presence of very close rings (between 1.2 µm for the first ring and 2.67 µm for the last ring). At a reverse voltage of 500V, all the 22 field rings can be observed, along with an additional peak corresponding to the border of the main junction. This implies that the OBIC method successfully reveals all the rings at this voltage level.

The amplitude of the maximum doesn't increase much from one voltage to another. The distance between the peaks is in total accordance with the layout of the first four rings as shown in **Fig. 14** and in **Table 2**. This table gives the position of each ring based on its right lateral edge that is oriented towards the main junction when viewed from the cross-section depicted in **Fig. 12**. The OBIC signal amplitude is given for each right lateral edge. Comparing the data from **Table 2** and the OBIC profile shown in **Fig. 14**, each dip in the profile perfectly matches with the left lateral edge of each ring. All the data in the present table were extracted from diode biased under 500 V.

Table 2. Distance from the main junction for ring mask layout and respective OBIC signal values.

Ring number	**#1**	**#2**	**#3**	**#4**
Distance from main junction (µm)	2.7	5.47	8.31	11.22
OBIC signal	2.69	5.49	8.49	11.29

Conclusions

It has been shown that OBIC measurements are possible on devices made from WBG semiconductor materials. It is possible to perform high voltage measurements through the vacuum chamber. It shows the efficiency of the periphery protection and help the designer to optimize his design (combination of MESA, JTE, rings…) to obtain a higher Breakdown Voltage.

This paper also presents OBIC measurements performed on field rings protected bipolar diodes at different voltages. This enhanced test-bench has a well improved spatial resolution compared to the previous OBIC test-bench. JTE rings are directly observable in these experiments, even with narrow distances between each ring. It would be then interesting to complete this study by measurements at higher reverse bias under vacuum and therefore to be closed to the breakdown voltage of the device (1 700 V). It would be also interesting to study

these same diodes by other complementary characterization methods such as micro-Raman spectroscopy and DLTS.

This µ-OBIC setup could also be used for other wide-bandgap semiconductor materials like GaN, Ga_2O_3, Diamond…

Acknowledgments. The authors would like to thank SuperGrid Institute and CALY Technologies for providing medium and high voltage SiC devices and also for financial support the Caisse des Dépôts et Consignations (CDC) and BPI-France (FilSiC: Convention n°O13953-410188).

References

[1] K. Shenai, R. Scott, B.J. Baliga, "Optimum Semiconductors for high-power electronics" IEEE Transactions on Electron Devices, Vol. 36, n°9, pp. 1811-1823, 1989.

[2] C. Raynaud, D. Tournier, H. Morel, D. Planson, "Comparison of high voltage and high temperature performances of wide bandgap semiconductors for vertical power devices" Diamond & Related Materials vol.19 p. 1-6, 2010.

[3] T. Mizushima, K. Takenaka, H. Fujisawa, T. Kato, S. Harada, Y. Tanaka, M. Okamoto, M. Sometani, D. Okamoto, N. Kumagai, S. Matsunanaga, T. Deguchi, M. Arai, T. Hatakeyama, Y. Makifuchi, T. Araoka, N. Oose, T. Tsutsumi, M. Yoshikawa, K. Tatera, A. Tanaka, S. Ogata, K. Nakayama, T. Hayashi, K. Asano, M. Harashima, Y. Sano, E. Morisaki, M. Takei, M. Miyajima, H. Kimura, A. Otsuki, Y. Yonezawa, K. Fukuda, H. Okumura and T. Kimoto, "Dynamic Characteristics of large current capacity module using 16-kV Ultrahigh voltage SiC Flip-type n-channel IE-IGBT" Proc. Int. Symp. On Power Semiconductor Devices & IC's, pp 277-280, 2014.

[4] J. Millán, P. Godignon, X. Perpiñà, A. Pérez-Tomás, J. Rebollo, "A Survey of Wide Bandgap Power Semiconductor Devices" IEEE Transactions on Power Electronics Year: Volume: 29, Issue: 5 Pages: 2155 – 2163, 2014

[5] K. Fukuda, D. Okamoto, M. Okamoto, T. Deguchi, T. Mizushima, K. Takenaka, H. Fujisawa, S. Harada, Y. Tanaka, Y. Yonezawa, T. Kato, S. Katakami, M. Arai, M. Takei, S. Matsunaga, K. Takao, T. Shinohe, T. Izumi, T. Hayashi, S. Ogata, K. Asano, H. Okumura, T. Kimoto, "Development of Ultrahigh-Voltage SiC Devices" IEEE Transactions on Electron Devices, Volume: 62, Issue: 2, Pages: 396 – 404, 2015.

[6] N. Kaji, H. Niwa, J. Suda, T. Kimoto, "Ultrahigh-Voltage SiC p-i-n Diodes With Improved Forward Characteristics", IEEE Transactions on Electron Devices, Volume: 62, Issue: 2, Pages: 374 – 381, 2015.

[7] R. Perret, Power Electronics Semiconductor Devices, Ed. Wiley-ISTE, ISBN: 978-1-848-21064-6, 2009.

[8] W. J. Choyke, H. Matsunami, G. Pensl, "Silicon Carbide: Recent Major Advances", Ed. Springer Science & Business Media, ISBN: 978-3-642-18870-1, 2003.

[9] P. Godignon, J. Montserrat, J. Rebollo, D. Planson "Edge Terminations for 4H-SiC Power Devices: A Critical Issue" Materials Science Forum Vol. 1062, pp 570-575, 2022.

[10] R. Stengl, "High-voltage planar junctions investigated by the OBIC method", IEEE Transactions on electron devices, vol. ED-34, no. 4, pages 911-919, 1987.

[11] T. Flohr and R. Helbig, "Determination of minority-carrier lifetime and surface recombination velocity by Optical-Beam-Induced-Current measurements at different light wavelengths," J. Appl. Phys., Vol. 66, Issue 7, pp. 3060-3065, 1989.

[12] C. Raynaud, D.-M. Nguyen, N. Dheilly, D. Tournier, P. Brosselard, M. Lazar, D. Planson "Optical beam induced current measurements: principles and applications to SiC device characterization", Phys. Status Solidi A 206, n°10, 2273-2283, 2009.

[13] D. Planson, P. Brosselard, K. Isoird, M. Lazar, L.-V. Phung, C. Raynaud, D. Tournier "Wide Bandgap Semiconductors for Ultra-High Voltage Devices. Design and characterization aspects". CAS Conference Sinaia - Romania 13-15 Octobre, 2014.

[14] D. Planson B. Asllani, L.-V. Phung, P. Bevilacqua, H. Hamad "Experimental and simulation results of optical beam induced current technique applied to wide bandgap semiconductors". Materials Science in Semiconductor Processing Vol. 94, pp 116-127, 2019.

[15] C. Sonneville, D. Planson, L.-V. Phung, P. Bevilacqua, B. Asllani "Interest of using a micro-meter spatial resolution to study SiC semi-conductor devices by Optical Beam Induced Current (OBIC)", Materials Science Forum Vol. 1004, pp 290-298, 2020.

[16] D. Planson, C. Sonneville, P. Bevilacqua, L V Phung, B. Asllani, D. Tournier, P. Brosselard "4H-SiC PiN diode protected by narrow fields rings investigated by the OBIC method", Materials Science Forum Vol. 1062, 2022.

[17]